

# Review Article : Applicable methods of evaluating peak area of gamma ray spectra

Thaer Laftah Al-Musawi, Shawkat Ismael Jubair, Zakariya Yahia Sulaiman

Department of Physics, college of Science, University of Baghdad, Baghdad, Iraq

[shawkat.jubair@sc.uobaghdad.edu.iq](mailto:shawkat.jubair@sc.uobaghdad.edu.iq)



## ARTICLE INFO

Received: 29 / 10 / 2022  
Accepted: 20 / 11 / 2022  
Available online: 22 / 12 / 2022

DOI: [10.37652/juaps.2022.176474](https://doi.org/10.37652/juaps.2022.176474)

### Keywords:

peak area,  
Gaussian shape,  
ROI,  
FWHM,  
asymptote,

## ABSTRACT

Gamma ray spectra have interesting information about energy and intensity of gamma photons. Normally, this information is available in the peak area and background region. A full energy peak sits on a background continuum and produced by full energy absorption of high energy photons, while background region is produced by Compton scattering of the photons. The most essential concern of errors is in the method of determining the events in both peak and background areas. The uncertainty is low when the background counts are small relative to the peak counts. However, it becomes high when the counts of the peak area are low with respect to that of background. The detection threshold for the peak is ultimately determined by the uncertainty in the background counts. This depends on the technique used and the form of the produced spectra. This paper reviews different methods of determining peak area and their associated uncertainties in terms of the principle and application of the techniques used.

## 1- Introduction

In gamma ray spectroscopy, the measurements depend on the counting of interactions of gamma rays with a detector where the gamma photons deliver part or all their energy into the sensitive part of the detector [1]. The output of these interactions is a spectrum which has important information concerning energy and intensity of radioisotope gamma photons [2].

Normally, the spectrum is composed of separated peaks, which are produced by full energy events, sit on top of a varying background continuum produced by Compton scattering. However, the most fundamental concern is the accuracy of determining peak areas and their associated error by subtraction the background continuum. When the peak to the background counting ratio is a high, the uncertainty is a small, while the error becomes great when the ratio is very small (less than 1). High peak counting with a low background counting is a good indication of propitiate peak area.

A Gaussian function is typical model used to represent the actual probability of distribution of the events in the peak area [3]. A full energy peak normally sits on several channels symmetrically in Gaussian shape where the position of the peak is in the centre. The peak position can be obtained by fitting a Gaussian approximation over the top two thirds or upper half of the peak area.

A Gaussian function can be used to define the full energy peak as follows

$$y(x) = y_0 \exp[-(x-x_0)^2/2\sigma^2] \dots\dots\dots(1)$$

where  $y(x)$  is the number of events in channel  $x$ ,  $y_0$  is the peak amplitude,  $x_0$  is the peak centroid and  $\sigma^2$  is the variance. The variance is a function of the full width at half maximum (FWHM) that can be written as

$$FWHM = 2\sqrt{2 \ln 2} \sigma = 2.354822 \ln 2 \sigma \dots\dots (2)$$

The upper description represents a special case of a normal distribution of events in peak area with no background.

For ideal case, full energy peaks are not precisely in a Gaussian shape, but in fact, they are sitting on a relatively high background continuum with a deviation in the low energy end (also named tailing) of the peak. Calculation of net counting of the peak area requires subtraction of the background. The

\*Corresponding author at :Department of Physics, college of Science, University of Baghdad, Baghdad, Iraq; ORCID: <https://orcid.org/0000-0000-00000->;Tel: E-mail address: [shawkat.jubair@sc.uobaghdad.edu.iq](mailto:shawkat.jubair@sc.uobaghdad.edu.iq)

accuracy of measuring the counts is seriously degraded when a fluctuation in the background counts occurs that establishes the limit of detection.

To improve the limit of detection of gamma ray spectroscopy, appropriate method for evaluating energy window should be considered. This article discusses a wide range of applicable approaches of determining peak area events and the effect of the uncertainty of counting statistics produced by Compton continuum.

## 2-Methods of evaluating peak area

The peak area is the measurement of the size of the region of interest, as shown by the peak in the spectrum. It depicts the variation in allowable pulse heights (energy) between the top and lower value. The area which is expressed in keV or MeV, can be configured automatically by the detecting system software which is time and effort saver and enables to investigate multiple peaks of the same spectrum or manually by the operator which takes longer time and more efforts [4]. Normally, it sets over peaks of specific one or more radionuclides to evaluate the total number of counting in the area. The area can also be specified for Compton or the region that combines Compton and peak region.

A precise peak area is needed for obtaining accurate statistics with raising the system's limit of detection. Ideal areas should wide enough to avoid the statistical inaccuracy which comes from low counts or Compton region and peak overlap [5].

### 3-1-Full Width at Half Maximum

The full width at half maximum (FWHM) of a peak, denoted by  $\Gamma$ , is a width of a peak with a counting is at half maximum value and measured in keV or channel [6]. It is a simple method used to determine total counts in the peak area [7, 8]. The procedure is achieved by identifying the central channel (centroid) of the peak that contains the highest count number. One or more channels on both sides of the peak that contain approximately half the number of the central channel counts is identified (Figure 1). The peak area counts are calculated by taking a vertical line from either side of the peak and intersecting it on the scale of energy [4]. This method gives a relatively low counting statistics, in which it integrates about 76% of the counts in the peak area [9].

Twice full width at half-maximum, 2(FWHM), is another method with procedure similar to that of FWHM. It is achieved by taking a twice the FWHM window. The peak area is set symmetrically relative to the centroid. The method is relatively more precise than FWHM method in which it integrates about 98% of the events in the peak [9].

There is also a Full Width at Tenth Maximum (FWTM), alternative approach for calculating peak area counts [10, 11]. Procedures of determining FWTM are similar to those of FWHM, while a tenth of the peak events are used to determine the peak area (Figure 1). Due to increased low-energy tailing in a peak brought on by charge trapping, the FWTM is considered as a stronger indicator of radiation dosimetry to the detector than the FWHM [12]. In this method, 95% of the peak events are integrated, but there is an intersection of the peak with Compton continuum in the low energy tail [9].

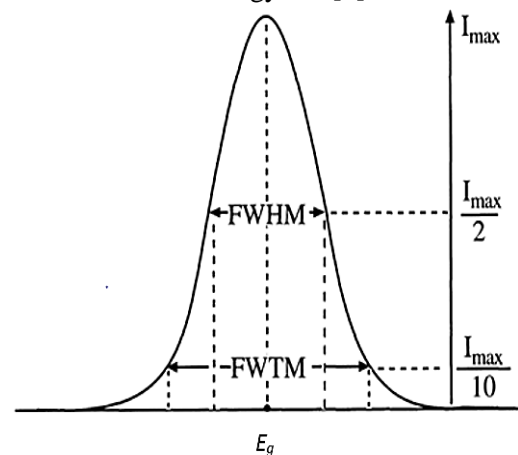


Figure 1: Calculation of FWHM and FWTM

### 3-2- Figure of Merit

Figure of Merit (FOM) or so called maximising events is a way used for determining peak area [13]. This method depends on maximizing the events in the peak area relative to that of background by successively adding symmetrical channel(s) on either halves of the peak reaching the widest possible area [14]. By drawing a histogram of the ratio between the highest and minimum amplitudes of the digitalized pulses, the FOM may also be determined [15, 16]. FOM can be obtained using the following equation [17].

$$FOM = \frac{S^2}{B} \dots\dots\dots (3)$$

where  $S^2$  is the square of the peak events and B is the background counts.

This method is similar to that of FWHM in which part may consider with integrating nearly 76% of the counted events [9].

### 3-3- Asymptote

Asymptote is a graphical method depends on maximising the counts in the peak area asymptotically [18]. The process involves taking a small region located in the centre of the centroid, then increasing the events with respect to the peak width [9]. The number of the peak events (Y) may propose to be at its maximum value by using the following:

$$Y = a * (1 - \exp^{-bx}) \dots \dots \dots (4)$$

where x is the peak width, a is the asymptote value and b is a proposed integer. The peak events approach the maximum as the peak width approaches infinity.

The parameters and constants of the asymptote equation can be obtained using some functions such as Microsoft Excel with solver, MATLAB with Lsqcurvefit, and HYDRUS-1D with Marquardt–Levenberg optimization algorithm [19]. This method can cover about 90% of the detected peak events [9].

### 3-4- Simple Gaussian Fits

A simple Gaussian fit method is used to provide consistent peak areas for spectra obtained by scintillation detectors. This fitting can be applied for overlapped or unresolved peaks precisely, so that a Gaussian fit can be set to a wide FWHM of the peak to determine the energy area [3]. The area is easily calculated when the centroid location and FWHM are primarily calculated from a Gaussian fit or when there is a peak with a considerable low energy end formed by Compton scattering. The peak area can also be found using any of the original data points and equation (1) after transforming Gaussian function into a line that is fitting least-squares to find the centroid and the variance.

The mean values of the peak are calculated from several points near the centroid that give a reasonable value for the equation of the area.

An algorithmic background and component peaks are used to construct a peak fitting model. Lineshapes, which are mathematical functions, are used to specify the component peaks, and fitting parameters are used to allow a component peak to vary in a number of different ways, such as position, FWHM, area, Lorentzian character, degree of

asymmetry, and Gaussian character. To create an approximate representation of the original data envelope, sets of component peaks are combined together to obtain the sum of all component peaks [8]. New statistical approaches of Gaussian fitting have been presented for complex spectra [20, 21].

### 3-5- Region of Interest Sums

The region of interest (ROI) is an important method used to determine peak areas of well-resolved peaks by simply summing peak counts (above background region) to find the peak area. This method tries to avoid difficulties associated with defects in spectral fitting algorithms' peak shape models, so that the summing not taking into account small variations in peak shape and gives accuracy and direct estimation in peak area.

The peak area (A) can be written as:

$$A = PC - BC \dots \dots \dots (5)$$

where PC is counts of the peak and BC is the background counts.

$$S^2(A) = S^2(P) + S^2(B) = P + S^2(B)$$

The estimated variance  $S^2(A)$  of the total area varies with the method used for estimation the background counts. Values of B and  $S^2(A)$  were calculated according to various parameters of the background continuum's position and width to the peak area ratio [3].

The procedure adopts three ROIs in which two are used to define the low and high energy sides of a peak whereas the third one defines the peak area. The continuum level at the ROI's center is calculated using the mean count of each channel. For a Gaussian function, three times the FWHM of the function (99.96%) of the peak area falls within a region centred at peak centroid. So, Therefore, about 99.9% of the peak area should be obtained by a peak ROI three times the FWHM and continuum ROIS spaced symmetrically 3.5-4 times the FWHM apart. Moreover, the approximated area can be more precise when it is quite wide, while the accuracy decreased with increasing energy intervals. Therefore, a spectrum with a remarkable low or high energy side requires a broader peak, i.e more than three times the FWHM. The area should be fitted to a high rate spectrum (low resolution), because peak resolution becomes worse at high rates. Almost, equal widths of the ROIs give good results, so the ROIs for low energy

and reference pulser peaks can usually be broader than three times the FWHM [3].

**3-6- Compton Continuum Subtraction**

The background or Compton continuum subtraction is considered one of the most widely used approaches for evaluating peak areas. Under a full peak, the shape of the Compton continuum is not usually fixed. This shape is a result of the nature of gamma ray interactions with the target at a given energy [3].

**3-6-1- Straight Line**

A straight line, trapezoidal or Covell's method is a simple and fast method in which it supposes a straight line of background continuum under photopeaks [22]. It uses peak regions and associated errors to identify peaks that are present but caused by low background levels [23]. The method is widely used to determine resolved or overlapped peaks by approximate subtraction of the Compton region with a straight line from high to low energy tailings (figure 2). The ROI is not necessarily to be symmetrical with respect to the peak area or with similar widths. The subtracted background which is in trapezoidal shape can be written as:

$$B = [Y(F_p) + W(L_p)] (N_p/2) \dots \dots \dots (6)$$

where  $Y(F_p) = mF_p + b$

$$Y(L_p) = mL_p + b, \text{ here } m = (Y_h - Y_l)/(X_h - X_l)$$

$$\text{and } b = (X_h Y_l - X_l Y_h)/(X_h - X_l)$$

The variance of the background (B) is written as:

$$S^2(B) = \left(\frac{N_p}{2}\right)^2 \left[ K^2 \frac{B_h}{N_h^2} + (2 - K)^2 \frac{B_l}{N_l^2} \right] \dots \dots \dots (7)$$

where  $K = \frac{F_p + L_p - 2X_l}{(X_h - X_l)}$

The above equation can be applied only when there are statistical uncertainties in background regions of interest ( $B_h$  and  $B_l$ ) which are set unsymmetrically relative to the peak region. It is also used with best results for complicated spectra such as plutonium.

When the background ROIs are symmetrical or the peak is much greater than the background continuum, a small uncertainty will occur and it can be determined by:  $S^2(B_l) = B_l$  and  $S^2(B_h) = B_h$ .

However, when peak regions are equal to background or less, a significant uncertainty is the most probable. The background and the variance are simplified i.e  $(F_p - X_l) = (X_h - L_p)$  and  $K = 1$ , and can be written as:

$$B = \left(\frac{Y_l + Y_h}{2}\right) N_p = \left(\frac{B_h}{N_h} + \frac{B_l}{N_l}\right) \frac{N_p}{2} \dots \dots \dots (8)$$

and

$$S^2(B) = \left(\frac{N_p}{2}\right)^2 \left(\frac{B_h}{N_h^2} + \frac{B_l}{N_l^2}\right) \dots \dots \dots (9)$$

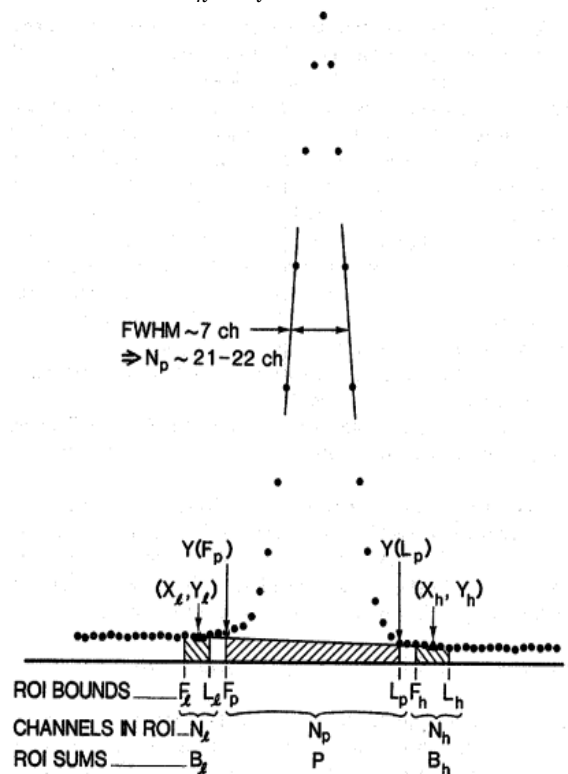


**Figure 2: Region of interest by background straight line subtraction.**

**3-6-2- Smoothed Step**

The smoothed step function or Savitzky-Golay's method is a method utilises the average of data to smooth them and minimise small scale oscillations [24]. It also functions with least square fittings process [23]. It takes part of Compton continuum, under a peak, produced by photons scattered with a small angle or full energy absorption of photons with incomplete charge collection [15].

According to the underlined spectral form, the genuine method is to produce a step function continuum under single or multiple peaks. Particularly for overlapping peak multiples, the method yields better results than the straight-line background approximation [25]. A logarithmic regression of a step function continuum is shown in figure 3. According to the notations in figure 2, the continuum at channel n is calculated by:

$$B_n = Y_l - D \left[ \frac{\sum_{i=x_l+1}^n (y_i - y_h)}{\sum_{i=x_l+1}^{X_h} (y_i - y_h)} \right] (10)$$

where  $y_i$  is the gross events in channel I,  $D = Y_l - Y_h$ ,  $B(X_l) = Y_l$  and  $B(X_h) = Y_h$ .

As the Compton counts of higher energy photons will not affect the figure of the smoothed step of lower energy photons, the background ( $Y_h$ ) is subtracted from each channel. The above formula can be applied for a background with a slight negative or no slope.

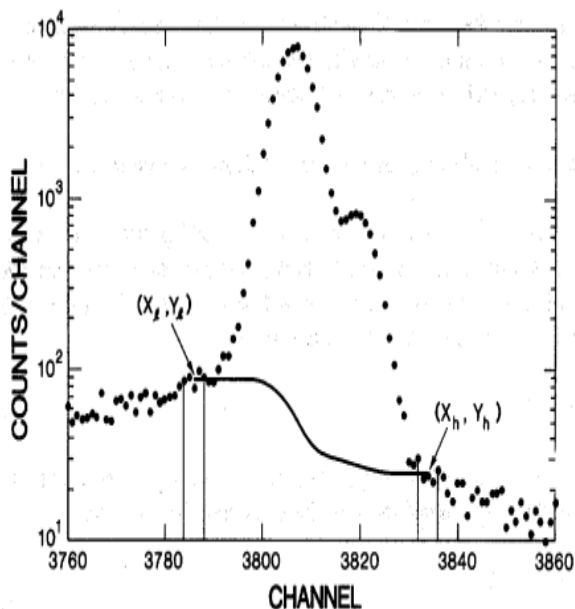


Figure 3: Region of interest by background smoothed line subtraction.

**4-6-3- Two Standard Procedures**

Two-standard procedure is a good application for background corrections when enriched U-235 is measured with the 185.7 keV energy photons and a single SCA window. It is also suitable to measure environmental contaminations at low concentrations of radioactive materials in water or other liquids [26]. In this method, the continuum is fixed, and the constant K of formula (13) is calculated precisely.

The equation of enriched energy can be written as:

$$E = C(P - KB) \dots\dots\dots (16)$$

here C is a constant takes per cent units ( $^{235}\text{U}/\text{count}$ ).

Assumptions were reported for two samples with two distinct and known enrichments presented at equal times [3].

**3-6-3- Single Region of Interest**

Single ROI for background region estimation is often necessary for spectra obtained by scintillation detectors or single-channel analysers (SCAs) to measure a radioactivity from  $^{235}\text{U}$  enrichment or  $^{239}\text{Pu}$  holdup [3].

Background continuum is estimated a flat when the peak/background ratio is high, and the participation of the background to the peak can be written as:

$$B = \frac{N_p}{N_h} B_h \dots\dots\dots (11)$$

$$s(B) = \frac{N_p}{N_h} s(B_h) \dots\dots\dots (12)$$

The method is almost employed for poor resolution counters, and also for germanium detectors considering no significant continuum on the low energy tailing of the peak. When the background continuum has a constant slope over the energy range, formula (11) can be written as:

$$B = KB_h \dots\dots\dots (13)$$

where K is a constant operator related to the sample and changed from sample to another. Various techniques are now in use. The ROIs can be manually drawn on the co-registered magnetic resonance images (MRI) [27-29], placed in geometrical shapes [30-32], used as templates [31, 32], or delimited using the threshold of maximal count within the striatal area [33-35].

**3-7- Library least-squares (LLSs)**

Library least-squares (LLSs) are spectral analysis techniques used for estimating the counting of sample components and correcting them from background scatter contributions [36-38]. In this approach, it is possible to divide gamma ray spectra into two or more components and account for it as a linear combination of these components that is reference standards or reference spectra. This assumption is based on that a measured spectrum is a linear superposition of sample constituent contributions [39].

The LLS technique can be written as follows

$$R_{s,i} = \sum_{j=1}^n \alpha_j R_{j,i} + e_i \dots\dots\dots (14)$$

where  $R_{s,i}$  is the counting rate in a given channel in the entire spectrum,  $R_{j,i}$  is the counting rate in a given channel of a given component,  $\alpha_j$  is the factors of a given element and  $e_i$  is the uncertainty in a given channel due to statistical fluctuations [40].

The calculations of LLS are achieved by summing the squares of the deviations, that is lowering chi squares (hypothesis test to show statistical differences) and this is performed by reducing the minimized chi squares relative to the reference standards:

$$\chi^2_v = \sum_{i=1}^n e_i^2 / (m - n) \sigma_i^2 \dots\dots\dots (15)$$

here  $(m-n)$  is the value of degrees of freedom,  $e_i$  is the fluctuation in the a given channel and  $\sigma_i$  is the errors in that channel. The minimisation can be lowered by equating the derivatives with regard to the stored standards and making them close to zero.

Consideration has recently been given to the use of the LLS technique for scatter correction in gamma-ray tomography systems [40] as a result of its comparatively successful application for multiphase hydrocarbon flow measurement [41] and for characterization of sub-sea fluid samples [42] using prompt gamma-ray neutron activation analysis.

### 3-8- Complex Fitting Codes

They are computer software that contain codes employed to analyse single or multiple peaks of a spectrum or for multi-sample in one time with many variations to determine the ROI from complex and overlapped peaks [43]. The codes explain the peaks in a Gaussian figure that have either one or both the low energy tails and may high energy tails. The long energy tail is almost not considered in the ROI as it is produced from Compton scattering with a small angle and it is not included in high resolution spectra. Even with equivalent results, the energy tails are varied from code to code. The fitting code procedures include peak models and subtraction of background region which is also varied [44]. Examples for these systems' software are and FitzPeaks™ by JF Computing [45], Genie™ 2000 by Mirion (Canberra) Technologies [46] and GammaVision™ by Ortec™ [47] and others. They often work well on good quality spectra obtained by high resolution detectors.

Several intercomparison on these software were made by IAEA [48], but other comparisons of updated software to manual procedures showed that most automatic software offered trustworthy and good outcomes [43].

## 2- Conclusion

An accurate counting statistics with low uncertainties has raised the need to find an appropriate method for determining peak area counts and hence to raise the counting system's detection limit. This article presented a review of various methods being used depending on the technique used and the resulted spectra (table 1). A method of high peak total counts with low background counts that avoids errors of Compton region overlap with peak is considered

acceptable peak area that provides good counting statistics with low uncertainties [5].

Table 1: Principle and application of various techniques used for energy area determinations

	Method	Principle	Application
FWHM	FWHM	Graphical method (drawing vertical line from both sides of the peak and intersecting it with energy scale)	For broad Gaussian peaks of poor precision (76% integration)
	2FWHM	Same procedures to FWHM (taking twice FWHM)	For broad Gaussian peaks of poor precision (98% integration)
	FWTM	Same procedures to FWHM (taking one tenth of peak counts)	For broad Gaussian peaks of poor precision (95% integration)
	FOM	maximizing the events in the peak area relative to background	For Gaussian and well resolved peaks (76% integration)
	Asymptote	Graphical method (maximising the counts in peak area asymptotically)with analysis program	For Gaussian and well resolved peaks (90% integration)
	Simple Gaussian fit	1-Gaussian function to one fitted FWHM and a wide ROIS centered on each peak 2-centroid location and FWHM- a simple Gaussian fit to the middle 3-FWHM	1,2-for overlapped or unresolved peaks with low energy tailing 3-peaks with low energy tailing
	ROI sums	Dividing a peak into three ROIs (two for energy tails and the third for peak area)	For well-resolved peaks (99.9% integration)

Compton continuum subtraction			
	Two-standard procedure	Assuming background has a constant shape and constant factor of the element is known	Environmental contaminations at low concentrations
	Smoothed line	Producing a step function continuum under single or multiple peaks	for overlapping peak multiples
	Straight line	Supposing and subtraction straight line of background continuum under peaks	resolved or overlapped peaks
Complex Fitting Codes	Computer software with codes include peak models and background subtraction	For complex and overlapped peaks of single or multi-sample	
LLSs	Spectral analysis technique by dividing spectra into many components with reference standards	For unresolved peak multiples and recently for scatter correction	
Single ROI	ROIs can be delineated manually, placing geometrical shaped, using templates, or manually drawing	for poor resolution counters	

### 3- References

[1] Pomme, S., Fitzgerald, R. and Keightley, J., (2015). Uncertainty of nuclear counting. *Metrologia*, 52(3), p.S3.

[2] Cherry, S. R., Sorenson, J. A. and Phelps, M. E. (2012). *Physics in nuclear medicine*. 4<sup>th</sup> ed. Philadelphia, PA: Elsevier Health Sciences.

[3] ORTEC, E. (1985). Principles and applications of timing spectroscopy. Application Note AN-42.

[4] Knoll, G. F. (2010) Radiation detection and measurement. John Wiley & Sons Inc. USA.

[5] L' Annunziata M. (2012). Hand book of Radioactivity Analysis. 3rd Edition: Academic Press.

[6] Lee, M., Lee, D., Ko, E., Park, K., Kim, J., Ko, K., Sharma, M. and Cho, G., (2020). Pulse pileup correction method for gamma-ray spectroscopy in high radiation fields. *Nuclear Engineering and Technology*, 52(5), pp.1029-1035.

[7] Speakman, S.A., (2014). Estimating crystallite size using XRD. *MIT Center for Materials Science and Engineering*, 2, p.14.

[8] Major, G.H., Fairley, N., Sherwood, P.M., Linford, M.R., Terry, J., Fernandez, V. and Artyushkova, K., (2020). Practical guide for curve fitting in x-ray photoelectron spectroscopy. *Journal of Vacuum Science & Technology A: Vacuum, Surfaces, and Films*, 38(6), p.061203.

[9] Al-Musawi, T.L. (2018). Calibration of a scanning whole body counter for measurement of the activity of gamma emitting radionuclides in the human body. PhD thesis. Cardiff University.

[10] Asgari, A., Ashoor, M., Sohrabpour, M., Shokrani, P. and Rezaei, A., (2015). Evaluation of various energy windows at different radionuclides for scatter and attenuation correction in nuclear medicine. *Annals of Nuclear Medicine*, 29(4), pp.375-383.

[11] Evans, L.G., Boynton, W.V., Reedy, R.C., Starr, R.D. and Trombka, J.I., (2003). Background lines in the Mars Odyssey 2001 gamma-ray detector. In *X-Ray and Gamma-Ray Detectors and Applications IV* (Vol. 4784, pp. 31-44). SPIE.

[12] Kojima, A., Takaki, A., Noguchi, T., Matsumoto, M., Katsuda, N., Tomiguchi, S. and Yamashita, Y., (2005). Optimum energy window setting on Hg-201 x-rays photopeak for effective Tl-201 imaging. *Annals of nuclear medicine*, 19(7), pp.541-547.

[13] Lintereur, A.T., Ely, J.H., Stave, J.A. and McDonald, B.S. (2012). *Neutron and gamma ray pulse shape discrimination with polyvinyltoluene* (No. PNNL-21609). Pacific Northwest National Lab.(PNNL), Richland, WA (United States).

[14] Prekeges J. (2010). Nuclear Medicine Instrumentation. *Journal of Nuclear Medicine Technology*, 38(3), pp. 172-173.

[15] Knoll, G.F. (2010). *Radiation detection and measurement*. John Wiley & Sons.

[16] Balmer, M.J., Gamage, K.A. and Taylor, G.C., (2015). Comparative analysis of pulse shape

- discrimination methods in a  $^6\text{Li}$  loaded plastic scintillator. *Nuclear Instruments and Methods in Physics Research Section A: Accelerators, Spectrometers, Detectors and Associated Equipment*, 788, pp.146-153.
- [17] Kessler, M.J. ed. (1989). *Liquid Scintillation Analysis: science and technology*. Packard Instrument.
- [18] Crank, J., (1979). *The mathematics of diffusion*. Oxford university press.
- [19] Lee, C.P., Hu, Y., Chen, D., Tien, N.C., Tsai, S.C., Shi, Y., Lee, I.H. and Ni, C.F., (2021). A Statistical Evaluation to Compare and Analyze Estimations of the Diffusion Coefficient of Pertechetate ( $^{99}\text{TcO}_4^-$ ) in Compacted Bentonite. *Minerals*, 11(10), p.1075.
- [20] Li, Z., Tuo, X., Shi, R. and Yang, J., (2014). A statistical approach to fit Gaussian part of full-energy peaks from Si (PIN) and SDD X-ray spectrometers. *Science China Technological Sciences*, 57(1), pp.19-24.
- [21] Yang, Z., Li, Y., Yu, Q. and Qu, S., (2013). The application of the Levenberg-Marquardt gaussian fitting method in NaI (TI)  $\gamma$  spectrum analysis. *Nuclear Electronics and Detection Technology*, 33(10), pp.1271-1273.
- [22] Sterlinski, S., (1968). Analysis of digital data from a multichannel pulse height analyzer on gamma ray total absorption peaks in activation analysis. *Analytical Chemistry*, 40(13), pp.1995-1998.
- [23] Fearn, S.J., Kaluvan, S., Scott, T.B. and Martin, P.G., (2022). An Open-Source Iterative Python Module for the Automated Identification of Photopeaks in Photon Spectra. *Radiation*, 2(2), pp.193-214.
- [24] Savitzky, A. and Golay, M.J., (1964). Smoothing and differentiation of data by simplified least squares procedures. *Analytical chemistry*, 36(8), pp.1627-1639.
- [25] Gunnink, R., Evans, J. E. and Prindle, A. L. (1976). A Reevaluation of the Gamma-Ray Energies and Absolute Branching Intensities of  $^{237}\text{U}$ ,  $^{283,239,240,241}\text{Pu}$ , and  $^{241}\text{Am}$ . Lawrence Livermore Laboratory report UCRL-52139.
- [26] Gedcke, D.A. (2009). How counting statistics controls detection limits and peak precession. ORTEC Application Notes AN59. Website:/www.ortec-online.comS.
- [27] Chen, P.S., Yeh, T.L., Lee, I.H., Lin, C.B., Tsai, H.C., Chen, K.C., Chiu, N.T., Yao, W.J., Yang, Y.K. and Chou, Y.H. (2011). Effects of C825T polymorphism of the GNB3 gene on availability of dopamine transporter in healthy volunteers—a SPECT study. *Neuroimage*, 56(3), pp.1526-1530.
- [28] Chen, P.S., Yeh, T.L., Lee, I.H., Lin, C.B., Tsai, H.C., Chen, K.C., Chiu, N.T., Yao, W.J., Yang, Y.K. and Chou, Y.H. (2011). Effects of C825T polymorphism of the GNB3 gene on availability of dopamine transporter in healthy volunteers—a SPECT study. *Neuroimage*, 56(3), pp.1526-1530.
- [29] Hesse, S., Ballaschke, O., Barthel, H. and Sabri, O. (2009). Dopamine transporter imaging in adult patients with attention-deficit/hyperactivity disorder. *Psychiatry Research: Neuroimaging*, 171(2), pp.120-128.
- [30] Árgyelán, M., Szabó, Z., Kanyó, B., Tanács, A., Kovács, Z., Janka, Z. and Pávics, L. (2005). Dopamine transporter availability in medication free and in bupropion treated depression: a  $^{99\text{mTc}}$ -TRODAT-1 SPECT study. *Journal of affective disorders*, 89(1-3), pp.115-123.
- [31] Szobot, C.M., Shih, M.C., Schaefer, T., Júnior, N., Hoexter, M.Q., Fu, Y.K., Pechansky, F., Bressan, R.A. and Rohde, L.A. (2008). Methylphenidate DAT binding in adolescents with Attention-Deficit/Hyperactivity Disorder comorbid with Substance Use Disorder—a single Photon Emission Computed Tomography with [ $^{99\text{mTc}}$ ] TRODAT-1 study. *Neuroimage*, 40(3), pp.1195-1201.
- [32] Chiu, N.T., Lee, B.F., Yeh, T.L., Chen, P.S., Lee, I.H., Chen, K.C. and Yang, Y.K. (2011). Relationship between striatal dopamine transporter availability and sleep quality in healthy adults. *Molecular imaging and biology*, 13(6), pp.1267-1271.
- [33] Chen, P.S., Yang, Y.K., Yeh, T.L., Lee, I.H., Yao, W.J., Chiu, N.T. and Lu, R.B. (2008). Correlation between body mass index and striatal dopamine transporter availability in healthy volunteers—a SPECT study. *Neuroimage*, 40(1), pp.275-279.
- [34] Felicio, A.C., Godeiro-Junior, C., Shih, M.C., Borges, V., Silva, S.M., de Carvalho Aguiar, P., Hoexter, M.Q., Barsottini, O.G., Andrade, L.A., Bressan, R.A. and Ferraz, H.B. (2010). Evaluation of patients with Clinically Unclear



- Parkinsonian Syndromes submitted to brain SPECT imaging using the technetium-99m labeled tracer TRODAT-1. *Journal of the neurological sciences*, 291(1-2), pp.64-68.
- [35] Ziebell, M., Pinborg, L.H., Thomsen, G., de Nijs, R., Svarer, C., Wagner, A. and Knudsen, G.M. (2010). MRI-guided region-of-interest delineation is comparable to manual delineation in dopamine transporter SPECT quantification in patients: a reproducibility study. *Journal of nuclear medicine technology*, 38(2), pp.61-68.
- [36] Salmon, L., 1961. Analysis of gamma-ray scintillation spectra by the method of least squares. *Nuclear Instruments and Methods*, 14, pp.193-199.
- [37] Gardner, R.P., Sood, A., Wang, Y.Y., Liu, L., Guo, P., Gehrke, R.J., (1997). Single peak versus library least-squares analysis methods for the pgnaa analysis of vitrified waste. *Applied Radiation and Isotopes* 48, 1331–1335.
- [38] Gardner, R.P., Wielopolski, L., Verghese, K., (1978). Mathematical techniques for quantitative elemental analysis by energy dispersive x-ray fluorescence. *Journal of Radioanalytical Chemistry* 43, 611–643.
- [39] Melo, S.B., Meric, I., Silva, F., Dantas, C.C., Sølief, J.R., Johansen, G.A., Hjertaker, B.T. and Barros, B.J., (2017). A Geometric Approach to Spectral Analysis. *arXiv preprint arXiv:1711.07782*.
- [40] Meric, I., Johansen, G.A. and Moreira, I.V.M., (2015). A library least-squares approach for scatter correction in gamma-ray tomography. *Radiation Physics and Chemistry*, 108, pp.39-47.
- [41] Wang, J., Li, F., Gardner, R.P., (2008). On the use of prompt gamma-ray neutron activation analysis for determining phase amounts in multiphase flow. *Measurement Science and Technology* 19, 094005. doi:10.1088/0957-0233/19/9/094005.
- [42] Meric, I., Johansen, G.A., Holstad, M.B., Wang, J., Gardner, R.P., (2011). Produced water characterization by prompt gamma-ray neutron activation analysis. *Measurement Science and Technology* 22, 125701. doi:10.1088/0957-0233/22/12/125701.
- [43] Zahn, G.S., Genezini, F.A. and Morales, M., (2015). Evaluation of peak-fitting software for gamma spectrum analysis. *arXiv preprint arXiv:1511.04362*.
- [44] Helmer, R. G. and Lee, M. A. (1980). Analytical Functions for Fitting Peaks from Ge Semiconductor Detectors: *Nuclear Instruments and Methods* 178,499-512.
- [45] Fitzgerald, J.; *FitzPeaks Gamma Analysis and Calibration Software*. JF Computing Services. Available online: <https://www.jimfitz.co.uk/fitzpeak.htm> (July 2022).
- [46] Mirion Technologies, (Canberra) Inc. Genie™ 2000 Interactive Peak Fit. Available online: <https://www.mirion.com/products/genie-2000-interactive-peak-fit> (July 2022).
- [47] ORTEC® AMETEK Inc. GammaVision® 8.10, Gamma Spectroscopy Software. Available online: <https://www.ortec-online.com>. (July 2022).
- [48] Blaauw, M., Fernandez, V.O., Van Espen, P., Bernasconi, G., Noy, R.C., Dung, H.M. and Molla, N.I. (1997). The 1995 IAEA intercomparison of  $\gamma$ -ray spectrum analysis software. *Nucl. Instrum. Meth. A*, 387, pp.416-432.

## الطرق التطبيقية لحساب منطقة الذروة لأطياف اشعة كاما

ثائر لفته محسن الموسوي، شوكت اسماعيل جبير، زكريا يحيى سليمان

قسم الفيزياء، كلية العلوم، جامعة بغداد، بغداد، العراق  
[shawkat.jubair@sc.uobaghdad.edu.iq](mailto:shawkat.jubair@sc.uobaghdad.edu.iq)

### الخلاصة

تحتوي أطياف أشعة جاما على معلومات مثيرة للاهتمام حول طاقة وكثافة فوتونات اشعة جاما. عادة ، تكون هذه المعلومات متاحة في منطقة الذروة ومنطقة الاشعاعات الخلفية. تقع ذروة الطاقة الكاملة على سلسلة اشعاعات الخلفية المتصلة ويتم إنتاجها عن طريق امتصاص الطاقة الكاملة لفوتونات عالية الطاقة ، بينما تنتج منطقة اشعاعات الخلفية عن طريق تشتت كومبتون لفوتونات اشعة كاما. ان الجزء الاكبر للخطأ يكون متمثلاً في طريقة تحديد مناطق الذروة في كل من مناطق اشعاعات الذروة ومناطق الاشعاعات الخلفية. ان نسبة الخطأ تكون منخفضة عندما تكون كمية الاشعاعات الخلفية صغيرة بالنسبة لكمية اشعاعات الذروة. جوهرياً، فان عدم الدقة في حساب الاشعاعات الخلفية يقيد عملية حساب اشعة الذرة. ومع ذلك ، تكون نسبة الخطأ عالية عندما تكون كمية اشعاعات الذروة منخفضة مقارنة مع كمية الاشعاعات الخلفية. ان هذا يعتمد على التقنية المستخدمة وشكل الأطياف المنتجة. ان هذا البحث يستعرض طرقاً مختلفة لتحديد منطقة الذروة ونسبة الخطأ الناتجة من استخدام هذه الطرق طبقاً الى مبادئ وتطبيقات التقنيات المستخدمة.